R-spondin 2 mediates neutrophil egress into the alveolar space through increased lung permeability.

Sergio Randell Jackson
University of Pennsylvania
Maria Fernanda De Mello Costa
University of Pennsylvania
Christopher Frances Pastore
University of Pennsylvania
Gan Zhao
University of Pennsylvania
Aaron I. Weiner
University of Pennsylvania
Stephanie Adams
University of Pennsylvania
Gargi Palashikar
University of Pennsylvania
Kwaku Quansah
University of Pennsylvania
Kurt Hankenson
University of Michigan Medical School
De'Broski Herbert
University of Pennsylvania
Andrew Vaughan (andrewva@vet.upenn.edu)
https://orcid.org/0000-0001-5740-643X

Research note

Keywords: R-spondin 2, neutrophil migration, lung permeability, lung endothelial barrier, BALF, Wnt signaling, FITC-dextran, alveolar space

Posted Date: December 12th, 2019

DOI: https://doi.org/10.21203/rs.2.18790/v1

Version of Record: A version of this preprint was published on February 4th, 2020. See the published version at https://doi.org/10.1186/s13104-020-4930-8.

Abstract

Objective: R-spondin 2 (RSPO2) is required for proper lung morphogenesis. Our objective was to investigate whether RSPO2 is similarly important in homeostasis of the adult lung. Unexpectedly, we observed changes in neutrophil migration and lung vascular permeability in RSPO2-deficient ($RSPO2^{-/-}$) mice compared to RSPO2 control ($RSPO2^{+/+}$) mice, independent of experimental injury/challenge. Here we use multiple methods to quantify these observations to further understand how tonic RSPO2 expression regulates lung homeostasis.

Results: Quantitative PCR (qPCR) analysis demonstrated significantly higher myeloperoxidase (MPO) expression in bronchoalveolar lavage fluid (BALF) cell content from $RSPO2^{-/-}$ mice compared to $RSPO2^{+/+}$ mice. Immunocytochemical (ICC) analysis likewise demonstrated significantly more MPO+ cells in BALF from $RSPO2^{-/-}$ mice compared to $RSPO2^{+/+}$ mice, confirming the increase of infiltrated neutrophils. We then assessed lung permeability/barrier disruption via Fluorescein isothiocyanate (FITC)-dextran instillation and found a significantly higher dextran concentration in the plasma of $RSPO2^{-/-}$ mice compared to identically treated $RSPO2^{+/+}$ mice. These data demonstrate that RSPO2 may be crucial for lung barrier integrity and can facilitate an increase in neutrophil migration from circulation into alveolar spaces due to increased lung permeability/barrier disruption. Our studies suggest additional research is needed to evaluate RSPO2 in scenarios exhibiting either pulmonary edema or neutrophilia.

Introduction

Neutrophils are bone marrow-derived polymorphonuclear leukocytes that act as early responders to inflammatory stimuli (1–3). During a tissue injury, necrotic host cells release damage-associated molecular patterns (DAMPs), some of which act directly as chemoattractants to induce neutrophil migration to injured sites (3). DAMPs can also induce neighboring cells to release chemokines, including C-X-C motif chemokine ligand 8 (CXCL8), which is a main cytokine involved in the recruitment of neutrophils to inflammatory sites (3).

R-spondins are a family of four secreted agonists (RSPO1-4) of the canonical Wnt/β-catenin signaling pathway by acting as ligands for leucine-rich repeat-containing G-protein coupled receptors (LGRs) 4–5 receptors (4). RSPO2 is required for normal lung morphogenesis (5–7). Disruption of the RSPO2 locus results in severely hypoplastic lungs at birth, exhibiting > 50% reduction in lung weight (5). RSPO2 expression is largely restricted to the lung mesenchyme, suggesting a paracrine effect on the developing epithelium (5,8). Whether RSPO2 expression in the adult lung is physiologically relevant is unknown.

Lung permeability is a crucial marker for vascular endothelial status. Increased lung permeability has been shown to be present in chronic diseases, including acute respiratory distress syndrome (ARDS), cancer, and many inflammatory scenarios (9). Extravasation of water and small particles is believed to permeate between disrupted endothelial cells (10). FITC-dextran instilled in mice intranasally can be used

to detect changes in lung permeability, and the extent of permeability can be quantified by measuring the fluorescence concentration (ug/ml) in mouse blood plasma (11).

In this study, we demonstrate that RSPO2 deletion in adult mice results in the aberrant presence of neutrophils in the luminal space of the lung. Recognizing that lung neutrophils are normally restricted to capillaries and are activated and recruited into the interstitium or the alveolar parenchyma due to endothelial stress/damage (12), our study further demonstrates significant lung barrier dysfunction in $RSPO2^{-/-}$ mice, suggesting that tonic RSPO2 expression is required for normal barrier function. RSPO2 loss then further facilitates neutrophil egress from circulation into the alveolar regions. We thus identify an unexpected role of RSPO2 in the adult lung in regulation of neutrophil homeostasis and lung endothelial barrier maintenance.

Methods

Animals and treatment

All animal procedures were approved by the Institutional Animal Care and Use Committee of the University of Pennsylvania. For all experiments, 6- to 8-week-old, 17-to-20 g, inducible Cre (UBC-CreERT2) (13) (The Jackson Laboratory stock #007001), RSPO2 flox mice (a gift from Dr. Kurt Hankenson, University of Michigan) and C57BL/6 mice of both sexes were used in equal proportions. For all animal studies, no statistical method was used to predetermine sample size. The experiments were not randomized, and the investigators were not blinded to allocation during the experiments and outcome assessment.

Animal euthanasia

Mice were placed into a chamber and exposed to isoflurane (Midwest Veterinary Supply) concentration ≥ %5 until roughly one minute after breathing stopped. Cervical dislocation was then performed as a secondary method after isoflurane overdose. This method is approved by our IACUC committee.

Cre recombination

To induce CreERT2 recombination, three doses (1 mg/g body wt, days) of tamoxifen (TM) dissolved in 100 µl of Mazola® corn oil were administered via intraperitoneal injection to all mice ($RSPO2^{-/-}$ n = 3; $RSPO2^{+/+}$ n = 3; c57BL/6 n = 3) were treated at day 0 to 4. Primers used to detect Cre-recombination are as follows: Rspo2-floxA-Forward: ACTCTTACTGCCTGGGATCCTCATT, Rspo2-floxB-Reverse: CTTCTTCTGAGCACCATCTGC. To induce CreERT2 recombination in cultured lung fibroblasts, cells were treated with three doses (4 mM) of 4-Hydroxytamoxifen (4-OHT) dissolved in dimethyl sulfoxide (DMSO; Santa Cruz Biotechnology).

Lung fibroblast isolation and culture

Lung fibroblasts were isolated by inflating fleshly dissected mouse lungs with 15 U/mL dispase II (Gibco™) in Hank's Balanced Salt Solution (HBSS; Gibco™), tying off the trachea, cutting away lobes from the mainstem bronchi, placing them into dispase to incubate for 45 minutes shaking at room temperature and mechanically dissociated by pipetting in sort buffer (SB; Dulbecco's modified Eagle's medium (DMEM; Thermo Fisher Scientific) + 20% cosmic calf serum (CC; Thermo Fisher Scientific) + 5% 5,000 U/mL penicillin-streptomycin (P/S; Gibco™). After pelleting at 570 x g for 5 minutes at 4 °C, whole-lung suspension was treated with Red Blood Cell Lysis Buffer (Millipore Sigma) for 3 minutes, pelleted, and suspended in SB + 1:1000 DNase I (Millipore Sigma) for a 45 minutes recovery period shaking at 37 °C. Whole-lung suspension was then pelleted and suspended in SB.

1×10^7 cells were plated into a Corning® 6-well clear polystyrene flat-bottom microplate (Millipore Sigma) in DMEM + 20% CC + P/S and grown in a 37 °C incubator for 9 days without passaging with media changes roughly on days 3 and 6 before harvesting for mRNA or cytospins.

BALF collection

After the trachea was exposed, a 20-G catheter was inserted into the trachea for lavage. One milliliter of cold PBS was instilled into the mouse lungs followed by gentle aspiration repeated three times.

Immunofluorescence

BALF and fibroblast cytospin slides were blocked and stained in a solution of PBS + 1% BSA (Affymetrix), 5% nonimmune horse serum, 0.1% Triton X-100, and 0.02% sodium azide. Slides were blocked for 1 hour at 4 °C. Slides were then incubated in primary antibodies as listed below in blocking buffer overnight at 4 °C. Slides were then washed three times with cold PBS + 0.1% Tween-20 (Millipore Sigma) and subsequently incubated with secondary antibodies as listed below for > 2 h at room temperature. Slides were then washed three times in PBS prior to 1 μM DAPI (Life Technologies) incubation for five minutes and mounted with Prolong Gold (Life Sciences).

The following primary antibodies were used for immunofluorescence: goat anti-myeloperoxidase (MPO) (1:200 dilution; R&D Systems), rabbit anti-RSPO2 (1:200 dilution; Proteintech). The following secondary antibodies were used for immunofluorescence: Alexa Fluor 488-conjugated donkey anti-goat (1:1000, Thermo Fisher Scientific), Alexa Fluor 568-conjugated donkey anti-rabbit (1:1000, Thermo Fisher Scientific).

Quantification of BALF tissue immunofluorescence

To quantify MPO + cells, mosaic images covering entire BALF cytospins were generated from multiple 20 X fields captured on an upright fluorescence microscope (model DMi8, Leica) and tiled in LAS X software (Leica). The MPO + cells were manually counted, and the ratio of MPO + cells to DAPI + cells was calculated. At least three sections per slide ($RSPO^{-/-}$ n = 3; $RSPO^{+/+}$ n = 3), each containing ≥ 300 individual cells, were quantified for each mouse sample.

Quantitative PCR (qPCR) analyses and primers

RNA was isolated from both BALF and cultured fibroblasts using RNeasy™ (Qiagen). The amount of RNA input for cDNA synthesis was standardized within each experiment to the RNA isolate with the lowest concentration as measured by Nanodrop (Thermo Fisher Scientific). cDNA was synthesized using iScript™ Reverse Transcription Supermix (BioRad). RT-PCR reactions were performed using SsoAdvanced™ Universal SYBR® Green Supermix (Biorad) and run on an Applied Biosystems QuantStudio 6 Real-Time PCR System (Thermo Fisher Scientific).

Expression of each gene is relative to expression of mouse RPL37 (L37), RPL19 (L19), or glyceraldehyde 3-phosphate dehydrogenase (GAPDH) mRNA. The primer sequences are as follows GAPDH – Forward: AGGTCGGTGTGAACGGATTTG, Reverse: TGTAGACCATGTAGTTGAGGTCA, L37 – Forward: CTCGGAGGTTACGGGACTC, Reverse: CTTGCCCTCGTAGGTAATGGG, L19 - Forward: ATG TAT CAC AGC CTG TAC CTG, Reverse: TTC TTG GTC TCT TCC TCC TTG, MPO – Forward: AGTTGTGCTGAGCTGTATGGA, Reverse: CGGCTGCTTGAAGTAAAACAGG, and RSPO2 – Forward: AGACGCAATAAGCGAGGTGG, Reverse: CTGCATCGTGCACATCTGTT

FITC-dextran permeability assay

The permeability assay was performed as described in (11,14). Mice were anaesthetized with isoflurane and administered 40 µl FITC-dextran (10 mg/kg body weight) intranasally. After a 30-minute wait to allow FITC-dextran to circulate in the blood, blood was collected via cardiac puncture, and fluorescence intensity was determined using a spectrophotometer.

Cytospins

Collected BALF and harvested fibroblasts were centrifuged at 570 x g for 5 minutes, and the cells were suspended in 1 ml of PBS solution and fixed onto slides at 570 rpm for 4 minutes on a Cytospin 2 (Shandon).

Statistical Analysis

All statistical calculations were performed using Graphpad Prism. Mann-Whitney test was used to determine significance. A P value of less than 0.05 was considered significant.

Results

Infiltration of neutrophils into bronchoalveolar lavage fluid following RSPO2 deletion

We confirmed successful Cre-recombination of the RSPO2 gene in adult mice after TM treatment (Fig. 1a), and after 4-OHT treatment in vitro (Figs. 1c-d). While examining these mice to assess any potential impacts on lung homeostasis, we unexpectedly observed MPO-expressing cells, a definitive neutrophil marker (15), in the BALF of RSPO2$^{-/-}$ mice at a significantly higher percentage compared to

RSPO2$^{+/+}$ mice. qPCR analysis demonstrated significantly higher MPO expression in BALF cells in RSPO2$^{-/-}$ mice compared to RSPO2$^{+/+}$ mice (Fig. 2a). ICC analysis likewise demonstrated significantly more MPO + cells in the BALF of RSPO2$^{-/-}$ mice (Figs. 2b-c), confirming the increase of infiltrated neutrophils. Thus, RSPO2$^{-/-}$ mice exhibit elevated neutrophil egress into the alveolar space compared to RSPO2$^{+/+}$ mice in terms of both increased MPO-expressing cells and higher MPO mRNA expression in BALF.

RSPO2 deletion increases lung barrier permeability

Because neutrophils must exit circulation through the vasculature before eventual translocation into the alveolar lumen (12), we hypothesized that RSPO2 deletion might induce endothelial disruption to facilitate the observed egress of neutrophils into the bronchoalveolar space. To assess lung permeability resulting from endothelial disruption, we administered FITC-dextran via intranasal installation, a method used to assess lung permeability alterations (11,14,16), and measured resulting fluorescence in blood plasma after 30 minutes. A significant increase in plasma dextran concentration (ug/ml) was observed in RSPO2$^{-/-}$ mice compared to identically treated RSPO2$^{+/+}$ mice (Fig. 3a-b). Taken together, these data suggest that RSPO2 deletion increases lung barrier permeability.

Discussion

While RSPO2 expression in the embryonic lung mesenchyme is essential for proper lung development, whether RSPO2 expression in the adult lung is relevant in tissue homeostasis or repair is unknown. Our studies indicate an unpredicted role for RSPO2 expression in the lung as an important regulator of neutrophil homeostasis and lung barrier function. Deletion of RSPO2 induces pulmonary edema/vascular leak. We hypothesize that the combination of endothelial barrier dysfunction and a second unknown mechanism, likely involving neutrophil chemokine dysregulation, explains the appearance of neutrophils in particular in BALF of RSPO2$^{-/-}$ mice as opposed to a nonspecific accumulation of circulating immune cells. Further studies are needed to understand whether neutrophils are being actively recruited or whether they arrive in the alveolar space passively.

Based on developmental studies we presume the lung mesenchyme is the predominant source of RSPO2 and that RSPO2 acts primarily in a paracrine fashion, but this should be formally investigated. It is also possible that autocrine RSPO2 deletion in the endothelium could lead to the vascular leakiness phenotype. Moreover, RSPO2 deletion in the neutrophils themselves could cause spurious activation. Given the well described role of R-Spondins in potentiating Wnt signaling, we presume dysregulation of Wnt is the likely driver behind these phenotypes, which will again require further study. Our findings here indicate careful, cell type-specific studies should be performed to elucidate the range of RSPO2 functions in the adult lung and beyond.

Our studies indicate RSPO2 expression in the adult mouse regulates lung barrier function and neutrophil accumulation in the alveolar airspace. Further investigations at the molecular level will be necessary to

shed more light on the mechanisms of RSPO2 (or other R-Spondin family members) by which RSPO2 may regulate neutrophil chemoattractants and alter lung barrier function, as well as to determine whether RSPO2 is involved in inflammatory lung diseases. Our data support a model in which RSPO2 might serve as a negative regulator of the migration and function of neutrophils. Ultimately, these initial findings should seed larger efforts to elucidate specific roles for RSPO2 in lung homeostasis and lung disease.

Limitations

Since we utilized a global UBC-CreERT2 model to delete RSPO2, our studies cannot identify the most relevant cellular producers of RSPO2. Moreover, RSPO2 itself is a secreted, diffusible factor. As such, it is difficult to know either the cellular source of RSPO2 or the cell types(s) responding to RSPO2 signals. Future studies should use careful lineage-specific deletion to address these limitations.

Declarations

Ethics approval

All studies were approved by the University of Pennsylvania's Institutional Animal Care and Use Committees, protocol 806262, and followed all NIH Office of Laboratory Animal Welfare guidelines. No human / patient studies were performed.

Availability of data and materials

All data generated or analyzed during this study is included in this published article. Accompanying unprocessed, raw data is available from the corresponding author on reasonable request.

Funding

This work was supported by NIH Grant Number R00HL131817. The content is solely the responsibility of the authors and does not necessarily represent the official views of the National Institutes of Health. The funding body, NIH, did not play a role in the design of the study, the collection, analysis, and interpretation of data, or in writing the manuscript.

Acknowledgements

We thank Katherine M. Neupauer, Chetan Rane, Joseph N. Farschian, Yasaman Moharrer, Horace M. Delisser, and Kotaro Sasaki for their assistance in performing these studies. We acknowledge biorender.com for their free public domain vector lung and molecule illustrations used in this manuscript.

Consent for publication

No human studies were performed, so not applicable.

Competing interests

The authors declare no competing interests.

Authors' contributions

Conception and Design: S.R.J., M.F.D.M.C., and A.E.V; data acquisition: S.R.J., M.F.D.M.C., A.I.W., S.A., G.P., K.Q., and C.F.P; data analysis: S.R.J., M.F.D.M.C, C.F.P., G.Z., and A.E.V.; review and edit manuscript: S.R.J., M.F.D.M.C., K.H., D.H., and A.E.V. All authors read and approved the final manuscript.

Author information

Department of Biomedical Sciences, School of Veterinary Medicine, University of Pennsylvania, Philadelphia, PA 19104, USA

Sergio R. Jackson, Maria Fernanda De Mello Costa, Christopher F. Pastore, Gan Zhao, Aaron I. Weiner, Stephanie Adams, Gargi Palashikar, Kwaku Quansah, De'Broski R. Herbert, and Andrew E. Vaughan

Institute for Regenerative Medicine, University of Pennsylvania, Philadelphia, PA 19104, USA

Andrew E. Vaughan

Department of Orthopaedic Surgery, University of Michigan School of Medicine, Ann Arbor, MI 48109, USA.

Kurt Hankenson

Corresponding author

Andrew E. Vaughan

Abbreviations

4-OHT: 4-hydroxytamoxifen

ARDS: acute respiratory distress syndrome

BALF: bronchoalveolar lavage fluid

CC: cosmic calf serum

CXCL8: C-X-C motif chemokine ligand 8

DAMPs: damage-associated molecular patterns

DMEM: Dulbecco's modified Eagle's medium

DMSO: dimethyl sulfoxide

FITC: fluorescein isothiocyanate

HBSS: Hank's balanced salt solution

LGRs: leucine-rich repeat-containing G-protein coupled receptors

MPO: myeloperoxidase

P/S: penicillin-streptomycin

qPCR: quantitative PCR

RSPO2: R-spondin 2

$RSPO2^{-/-}$: R-spondin 2-deficient

$RSPO2^{+/+}$: R-spondin 2 control (wild type)

SB: sort buffer

TM: tamoxifen

UBC-CreERT2: inducible Cre

References

1. Németh T, Mócsai A. The role of neutrophils in autoimmune diseases. Immunol Lett. 2012;
2. El-Benna J, Hurtado-Nedelec M, Marzaioli V, Marie JC, Gougerot-Pocidalo MA, Dang PMC. Priming of the neutrophil respiratory burst: role in host defense and inflammation. Immunological Reviews. 2016.
3. Ng LG, Ostuni R, Hidalgo A. Heterogeneity of neutrophils. Nature Reviews Immunology. 2019.
4. Carmon KS, Gong X, Lin Q, Thomas A, Liu Q. R-spondins function as ligands of the orphan receptors LGR4 and LGR5 to regulate Wnt/β-catenin signaling. Proc Natl Acad Sci U S A. 2011;
5. Bell SM, Schreiner CM, Wert SE, Mucenski ML, Scott WJ, Whitsett JA. R-spondin 2 is required for normal laryngeal-tracheal, lung and limb morphogenesis. Development. 2008;
6. Yamada W, Nagao K, Horikoshi K, Fujikura A, Ikeda E, Inagaki Y, et al. Craniofacial malformation in R-spondin2 knockout mice. Biochem Biophys Res Commun. 2009;
7. Jin YR, Turcotte TJ, Crocker AL, Han XH, Yoon JK. The canonical Wnt signaling activator, R-spondin2, regulates craniofacial patterning and morphogenesis within the branchial arch through ectodermal-mesenchymal interaction. Dev Biol. 2011;
8. Hussain M, Xu C, Lu M, Wu X, Tang L, Wu X. Wnt/β-catenin signaling links embryonic lung development and asthmatic airway remodeling. Biochimica et Biophysica Acta - Molecular Basis of

Disease. 2017.
9. Mammoto A, Mammoto T, Kanapathipillai M, Yung CW, Jiang E, Jiang A, et al. Control of lung vascular permeability and endotoxin-induced pulmonary oedema by changes in extracellular matrix mechanics. Nat Commun. 2013;
10. Radu M, Chernoff J. An in vivo assay to test blood vessel permeability. J Vis Exp. 2013;
11. Chen H, Wu S, Lu R, Zhang YG, Zheng Y, Sun J. Pulmonary permeability assessed by fluorescent-labeled dextran instilled intranasally into mice with LPS-induced acute lung injury. PLoS One. 2014;
12. Maas SL, Soehnlein O, Viola JR. Organ-specific mechanisms of transendothelial neutrophil migration in the lung, liver, kidney, and aorta. Frontiers in Immunology. 2018.
13. Ruzankina Y, Pinzon-Guzman C, Asare A, Ong T, Pontano L, Cotsarelis G, et al. Deletion of the Developmentally Essential Gene ATR in Adult Mice Leads to Age-Related Phenotypes and Stem Cell Loss. Cell Stem Cell. 2007;
14. cummings steven M. Fluorescein Isothiocyanate (FITC) Labelled Dextran As A Peripheral Marker Of Lung Inflammation. In 2011.
15. Lau D, Mollnau H, Eiserich JP, Freeman BA, Daiber A, Gehling UM, et al. Myeloperoxidase mediates neutrophil activation by association with CD11b/CD18 integrins. Proc Natl Acad Sci U S A. 2005;
16. Rane CK, Jackson SR, Pastore CF, Zhao G, Weiner AI, Patel NN, et al. Development of solitary chemosensory cells in the distal lung after severe influenza injury. Am J Physiol - Lung Cell Mol Physiol. 2019;

Figures

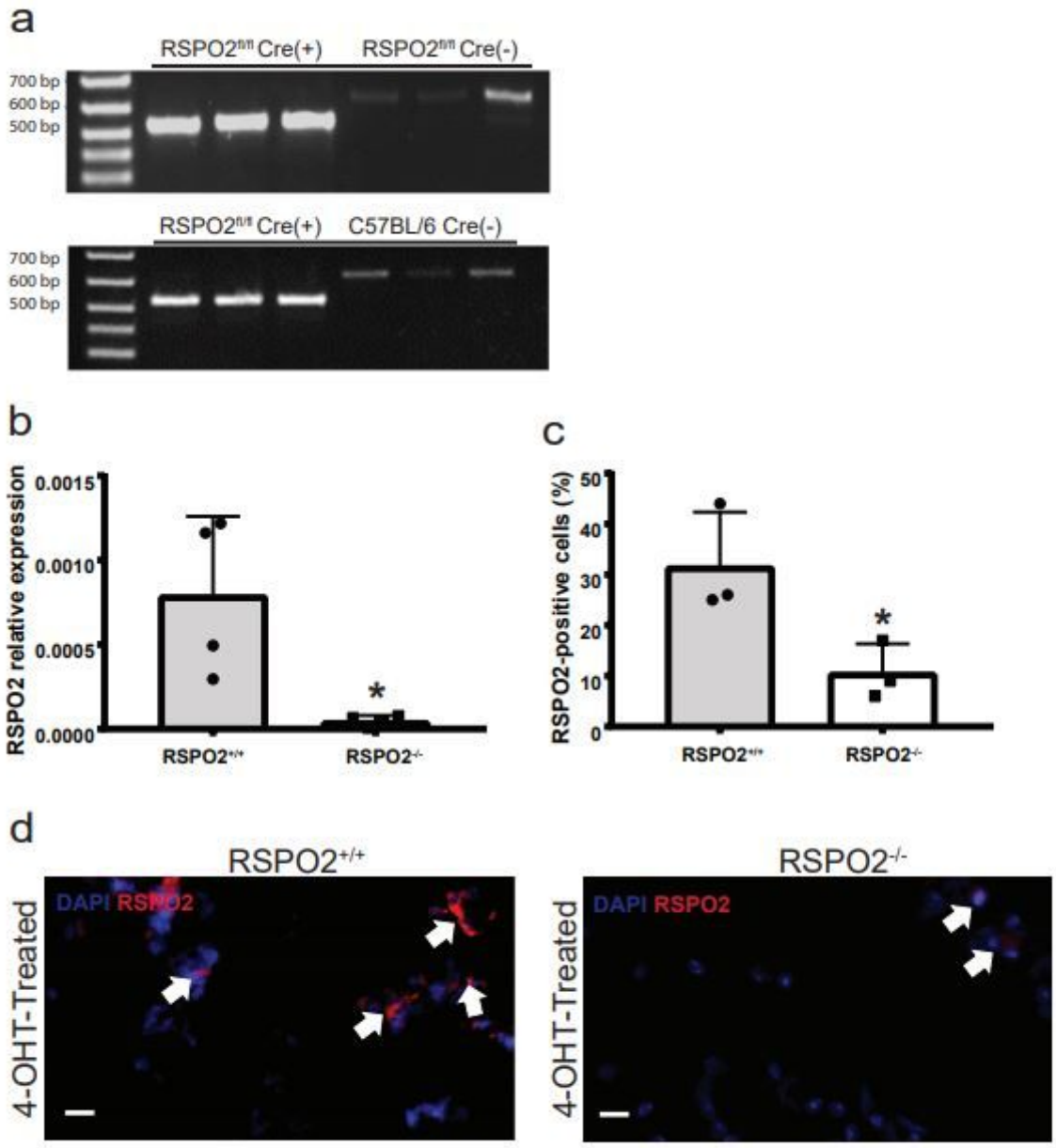

Figure 1

RSPO2 gene expression in lung homogenates from (a) RSPO2fl/fl;UBC-Cre-ERT2(+), RSPO2fl/fl;UBC-Cre-ERT2(-), and C57BL/6 mice post TM treatment. Cre-recombination of the loxP sites yields a 512 bp fragment, whereas the wild type allele yields a non-specific 600 bp fragment. qPCR analysis of (b) RSPO2 expression in the cultured fibroblasts isolated from the lungs of RSPO2-/- and RSPO2+/+ mice. Quantification of immunocytochemical evidence of (c-d) RSPO2 expression in fibroblasts isolated from RSPO2-/- and RSPO2+/+ mice. An arrow indicates examples of DAPI/RSPO2-double stained cells. Representative images are shown from RSPO2+/+ mice (n = 3) and RSPO2-/- mice (n=3) samples. * = A P value of less than 0.05 was considered significant.

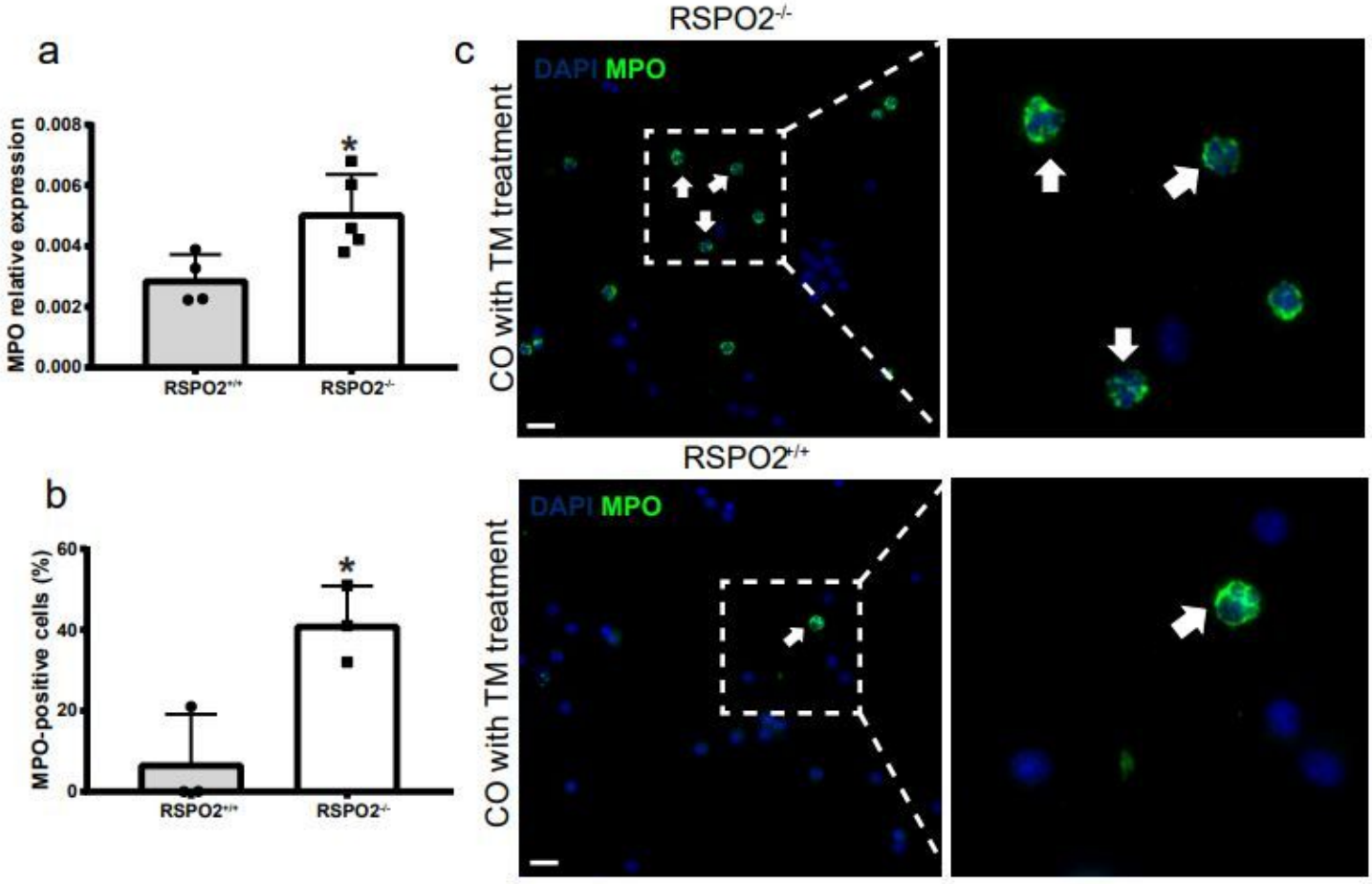

Figure 2

qPCR analysis of MPO expression in the BALF of (a) RSPO2-/- and RSPO2+/+ mice. Also shown is quantification of ICC of MPO expression in the BALF of (b-c) RSPO2+/+ mice and RSPO2-/- mice. An arrow indicates examples of DAPI/MPO-double stained cells. Representative images are shown from RSPO2+/+ mice (n = 3) and RSPO2-/- mice (n=3) samples. * = A P value of less than 0.05 was considered significant.

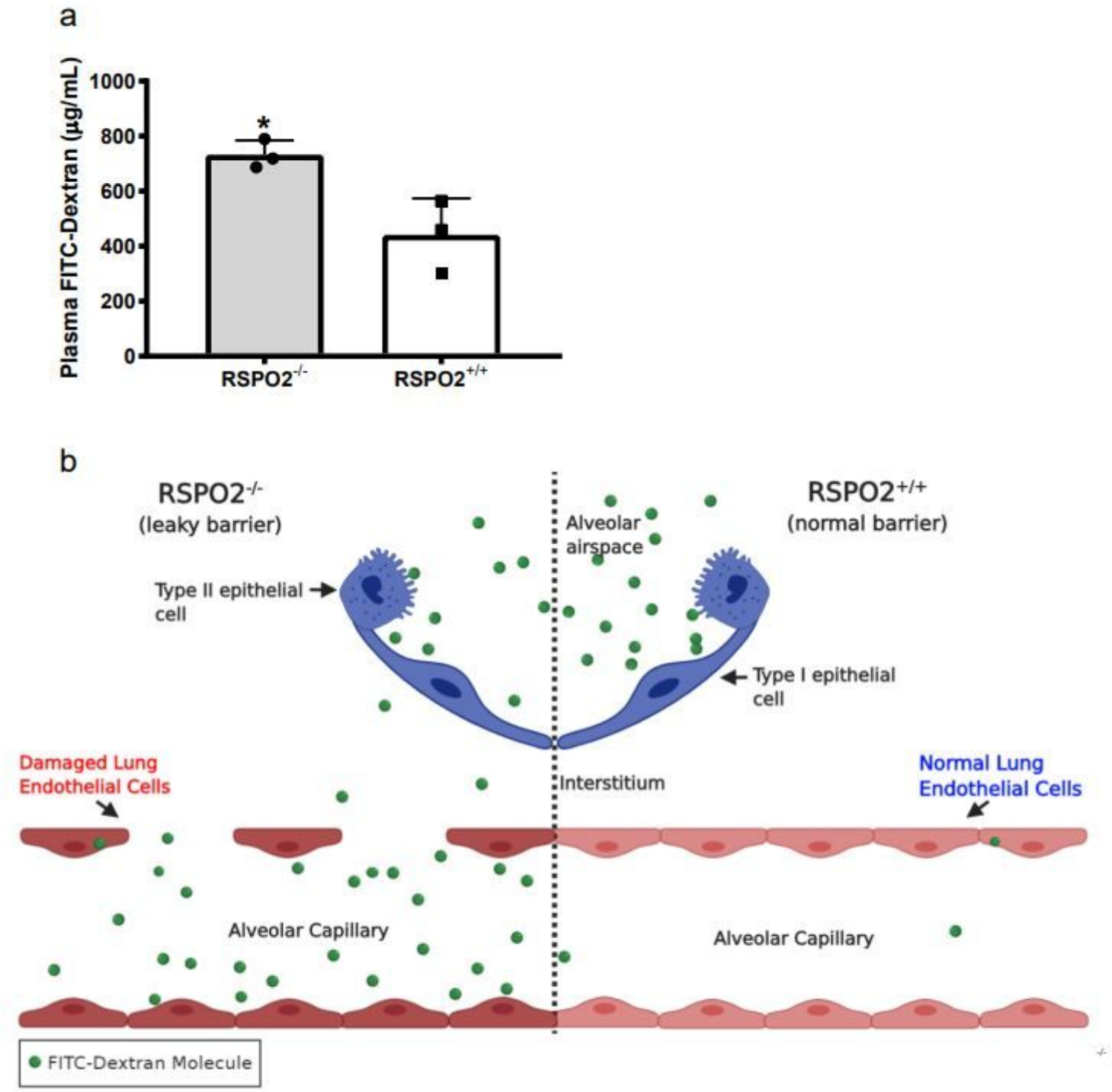

Figure 3

Lung permeability changes resulting from barrier disruption, as determined by a FITC-dextran assay. (a) A significant increase in average plasma dextran concentration (ug/ml) was observed in RSPO2-/- mice compared to identically treated RSPO2+/+ mice. (b) The movement of FITC-Dextran into normal alveolar capillaries (right side) and damaged alveolar capillaries (left side) during a murine model of endothelial cell barrier damage. Shown are the two crucial cell barriers, epithelial cells and endothelial cells. After intranasal instillation of FITC-Dextran solution, FITC-labeled molecules travel through the interalveolar

space and interstitium into alveolar capillaries. Each dot represents the average of each experimental group in each of n= 3 independent experiments. Statistical significance was demonstrated when mice from the control group and experimental group were averaged within each of the independent experiments, thus controlling for inherent variability in FITC-Dextran administration. When individual mice were pooled regardless of experiment, the results show a very similar trend as the averaged group, though not statistically significant. * = A P value of less than 0.05 was considered significant.

Supplementary Files

This is a list of supplementary files associated with this preprint. Click to download.

- NC3RsARRIVEGuidelinesChecklist1242019.pdf